On the optimization of the air source heat pump integration in high performance buildings

Alessandro Prada[1], Elena Bee[1], Andrea Gasparella[2], Paolo Baggio[1]
[1] Dep. of Civil, Environmental and Mechanical Engineering - University of Trento, Italy
[2] Faculty of Science and Technology - Free University of Bozen/Bolzano, Italy

Abstract

Air source heat pump coupled with PV panels is a promising solution for hydronic heating systems in high performance buildings. However, the configuration and operation of these systems must be properly designed considering the specific needs of high performance buildings. In the literature, several works dealt with the optimal coupling of HVAC systems in buildings but there is no agreement on the choice of the cost functions in the optimization problems.
This study presents an analysis on the extent to which the choice of the optimization objectives affects the design of a hydronic heating system in four reference buildings.

Introduction

The coming into force of the mandatory European Directive 2009/28/CE requires to increase the role of renewable energy sources to satisfy the energy consumptions of new buildings and major renovations. In this respect, the vapor-compression heat pump coupled with PV panels is a promising solution and, consequently, it is increasingly used for residential heating applications. This HVAC solution is especially advantageous in high performance building when low temperature hydronic systems are adopted. However, it has been observed that some issues arise in the control of the HVAC systems due to the fast changes in energy demand. Hence, the building might be easily subject to poor comfort conditions when the energy systems are installed in high performance houses which approach the nZEB target while maintaining economical convenience (Penna et al. (2015)). Besides, the seasonal performance of the heating system is strongly dependent on HVAC design, such as the system sizes (heat pump, water storage tank, PV battery), and on the adopted system control strategies. An optimal concurrent design of the HVAC and control systems installed in high performance building is essential to ensure the reduction of energy consumption and the achievement of thermal comfort for the entire heating season (Carlon et al. (2016)). In the literature, several works dealt with the optimal coupling of HVAC systems in buildings and some of them focus on high performance buildings. In the optimization problems different choices of cost functions can be done (Evins (2013)). Hasan et al. (2008) optimized the life cycle cost while Bichiou and Krarti (2011) added to this goal also the utility cost that is closely related to the energy consumption. Ihm and Krarti (2013) focused on energy savings and life cycle costs while Fesanghary et al. (2012) used life cycle costs and CO_2 emissions. Similarly, CO_2 savings and investment costs were adopted in other works (Hamdy et al. (2011a); Evins et al. (2012); Pountney (2012)). Thermal comfort is an objective that is often combined with the energy consumption. In this respect, PMV index (Magnier and Haghighat (2010); Eisenhower et al. (2012)), adaptive index (Hamdy et al. (2011b)), the number of discomfort hours (Asadi et al. (2014); Ascione et al. (2015); Wright et al. (2016)) or the long term discomfort indexes, like in Carlucci et al. (2013), are often adopted. Only few works used renewable coverage factor or sustainability indicators as optimization goals. For instance, Ko et al. (2015) added an index of renewable coverage in addition to economic and CO_2 targets. On the contrary, Wang et al. (2005) optimized the life cycle cost and life cycle environmental impact indexes while Verbeeck and Hens (2007) used life cycle assessment in addition to energy consumption and net present value.
This study presents an analysis on the extent to which the choice of the optimization objectives affects the design of an air source heat pump ($ASHP$) system installed in high performance buildings. The complex interactions among building, occupants, weather conditions and HVAC systems are considered by means of a dynamic simulation tool. Moreover, the trade-off solutions among different optimization objectives are evaluated by coupling the dynamic simulation tool with a genetic algorithm code developed in Matlab.

Method

Genetic Algorithm (GA) Implementation

In order to perform the multi-objective optimization (MOO) a genetic algorithm was developed in Matlab. The implemented GA is an Elitist Non-dominated sorting GA algorithms NSGA-II firstly proposed by

https://doi.org/10.26868/25222708.2017.090

Deb (2002). Nonetheless, several customizations of the code are used such as sampling, crossover, mutation, selection procedure and stopping criteria. These adjustments coupled with the selection of mutation rate, population size, crossover fraction are adopted with the purpose of increasing the GA performances. The first step in the GA procedure is the selection of the initial population. In this regard, random sampling could lead to an over-focus on same regions of the hyperspace without sampling in others, whereas a uniform random number generation produces uniform sample when the population size is high, as pointed out by Saltelli et al. (2004). For this reason, the code was complemented with a Sobol sequence sampling in order to overcome the clustering which can occur with sample random sampling or quasi random generator. Sobol sequence is a low-discrepancy sequence, which aims to give a uniform distribution of values in higher dimensions.The random starting point in the Sobol sequence was obtained through a pseudo-random generator proposed by Matsumoto and Nishimura (1998). Once the fitness function is evaluated, the GA proceeds with the selection of the best individuals. The selection is the procedure by which GA chooses parents for the next generation. In this study we adopted the tournament selection without replacement presented in Goldberg et al. (1989) and Goldberg and Deb (1990). In this method, a short list of four eligible parents are randomly chosen and the best individual out of that set to be a parent. Following on from this point, the code combines the genetic characteristics of both parents, giving rise to the new generation. The recombination procedures implemented is based on arithmetic weighting of parents genes to create children. Children are a random arithmetic mean of two parents, uniformly on the line between the parents (Burjorjee (2013)). The adopted crossover fraction, i.e. the fraction of the next generation produced by the crossover, was set to 0.8. The remaining individuals in the next generation becomes from mutation of population. Mutation is applied at a random point in a random individual. In particular, by means of Mersenne-Twister pseudo random generator, a randomly selected gene is replaced by a uniformly distributed random value that meet the gene range. The hypervolume measure, originally proposed by Zitzler and Thiele (1999), was used as a stopping criterion. Although with the drawback of the higher computational cost in the evaluation of the size of dominated space, the maximization of this index is the necessary and sufficient condition for the Pareto optimal solutions of a discrete MOO problem, as proved by Fleischer (2003).

Simulation layout

A coupled simulation of the house and its heating system was set up in the TRNSYS simulation suite. Standard and TESS libraries are used to model the building, storage tank, PV modules and battery systems, while the new subroutine proposed in Bee et al. (2016) was adopted to simulate the part load behavior of an inverter air source heat pump ($ASHP$). The simulations were carried out considering the weather data of Trento, that is a city in the Northern Italy having a $4A$ climate according to ASHRAE 90.1 (2007) classification. Moreover, several simplified reference buildings were investigated with the purpose of broaden the results validity. The semi-detached house presented in Prada et al. (2015) was modified in order to consider the influence of the insulation level and the thermal capacitance of the building envelope on the optimal coupling of the $HVAC$ system. For this reason, concrete block (C) and timber envelope (T) with either a low (1) or a high (2) insulation level were studied (Table 1).
The heating system is based on an $ASHP$, with variable speed compressor, coupled with radiant floor panels. The $ASHP$ part load operation is described by a performance curve defined in Bee et al. (2016) and depending on the capacity ratio (CR) according to the EN 14285 (2012). The performance curve provides the ratio of the part load COP normalized by the COP_{rated} given by the manufacturer starting from a full load test at the source temperatures of $7°\,C$ and $35°\,C$. Two points fully identify the change in the $ASHP$ operation at part-load. The first is the CR_{deg} where the COP begins to degrade due to the on/off cycles. The second is the CR_{max} value providing the maximum COP. An on/off controller with a dead-band ($DB_{HP,adj}$) turns the $ASHP$ off when it reaches the lower modulating limit and water is warmed up more than required. A water storage tank separates the circuit in the supply side, with the $ASHP$, and in demand side, with the circulation pump and radiant panel loops. The heating system is powered by either grid or photovoltaic (PV) electric power in an UPS like mode avoiding the batteries operation in parallel with the grid, according to the Italian legislation. Hence, the system is connected to the grid only when the battery has been completely discharged. The radiant floor design referred to a typical commercial configuration with a pipe spacing of 0.1 m and cross-linked polyethylene pipes having a diameter of $0.016\,m$, a thickness of $0.002\,m$ and a thermal conductivity of $0.44\,W\,m^{-1}\,K^{-1}$. The radiant panels supply temperature is adjusted according to an outdoor temperature reset curve defined by the minimum supply temperature $T_{supp,min}$ at the balance point and by the curve slope $s_{clim,adj}$.The water discharge is controlled by a thermostat with a proportional band (PB). The set point temperature of the ambient thermostat was set to $20\,°\,C$ while the set back temperature (T_{SB}) and the time to set back start (SB_{start}) and stop (SB_{stop}) are optimization variables.

Table 1: Envelope properties according to EN ISO 6946 and EN ISO 13786

Case	U [$\mathbf{W\,m^{-2}\,K^{-1}}$]	κ_{int} [$\mathbf{kJ\,m^{-2}\,K^{-1}}$]
Radiant Floor		
$C1$	0.80	50.9
$T1$	0.80	36.9
$C2$	0.29	50.6
$T2$	0.29	36.5
Wall and Ceiling		
$C1$	0.80	54.1
$T1$	0.80	30.4
$C2$	0.29	54.0
$T2$	0.29	31.1

Optimization Variables

Two different types of variables have to be optimized in order to improve the performance of an $HVAC$ system and to better design the coupling with the building. Firstly, the design variables affecting the $HVAC$ performance have to be correctly designed by considering the specific characteristics of the building construction and operation. In this respect, the variables optimized in this work were the sizes of the main components such as $ASHP$, storage tank, PV modules and batteries. Besides, the optimal tilt and orientation angles of the PV modules and the parameters of the part load curve of the $ASHP$ were also considered (Table 2). These variables affect the initial cost of the heating systems (IC) since they change the size and quality of the components. For this reason, starting from a market survey, the following regression curves were obtained for the estimation of the initial cost of the systems when the cost is used as an optimization goal.

$$IC_{ASHP} = COP_{rated}^{2.1305} \cdot (127.03 + 20.71 \cdot \phi_{rated})$$
$$IC_{stor} = 2.60 \cdot 10^{-3} \cdot V_{stor} + 456.4$$
$$IC_{PV} = 1550 + 862.5 \cdot n_{str}$$
$$IC_{batt} = 0.274 \cdot Q_{batt}^{0.9376} \cdot n_{batt}$$

Moreover, the variables governing the operation of the energy systems must be adjusted in order to increase the performances of the system. In this case, the modification of the $HVAC$ controls represents an energy saving measure without additional costs. In this research we considered the modification of the climatic adjustment curve, the deadband of the $ASHP$ thermostat, the PB of the ambient thermostat and the set back temperature and schedule (Table 2).

GA objectives

The fitness function of the GA code is a MatLab script that writes down the input file and launches TRNSYS model for the energy simulation. After the model execution, the script reads the TRNSYS outputs and post-processes the simulation results. Following on from this point, the code computes the optimization objectives and it returns them to the $NSGA-II$ algorithm. Four different objectives were adopted, since the aim of the work is to point out the effect of the objective choice on the optimal $HVAC$ configurations. The first objective index is the annual power consumption for heating (Q_h). This objective was calculated by summing for each timestep the energy required by the circulation pump and by the $ASHP$. The second objective is the PV self consumption (AC) that is closely related to the renewable coverage factor. This index computed the annual energy of the $ASHP$ and of the auxiliary systems that comes from the batteries or from the PV panels. This index is computed in TRNSYS by means of an equation and by an integration type. The third GA objective is the total number of unmet hours (UH) during the occupied periods. This index identifies the period of time in which the internal air temperature does not meet the set point due to the low $HVAC$ capacity or the high inertia of the heating system. This index is related to the thermal comfort perception since the air temperature is one of the four main variables of the PMV. Finally, the last GA objective is an economical index. In this respect, the net present value (NPV) is calculated to define economic benefits of each $HVAC$ configuration. This approach allows the analysis of different time series of cash flows related to each solution based on a lifespan that was considered equal to 30 years. The NPV takes into account the initial investment cost, the annual running costs, the maintenance cost, the replacement costs, and the residual value, according to the EN 15459 (2007). The initial cost were defined starting from a market survey, by defining a pattern of costs as

Table 2: Optimization variables

Variable	Units	Min	Max	Step
HVAC design variables				
V_{stor}	m^3	0.05	2.00	0.05
ϕ_{rated}	kW	4	14	0.2
COP_{rated}	-	2.5	5.0	0.1
CR_{deg}	-	0.20	0.40	0.05
CR_{max}	-	0.45	0.60	0.05
PV strings (n_{str})	-	1	8	1
PV tilt angle	deg	0	90	10
PV azimuth	deg	-90	90	45
Q_{batt}	Wh	108	2376	108
n_{batt}	-	1	4	1
HVAC control variables				
T_{supp_min}	$°C$	25	35	1
$s_{clim,adj}$	-	0	0.33	0.033
$DB_{HP,adj}$	$°C$	0.5	2.5	0.5
T_{SB}	$°C$	15	19	0.5
SB_{start}	h	19	23	1
SB_{stop}	h	5	8	1
PB	$°C$	0.5	1	0.5

Table 3: Optimization runs with the choice of different optimization goals

Code	Q_h	NPV	UH	AC
Opt1	x	x		
Opt2	x		x	
Opt3	x			x
Opt4		x	x	
Opt5			x	x
Opt6		x		x
Opt7	x	x	x	
Opt8	x	x		x
Opt9	x		x	x
Opt10		x	x	x
Opt11	x	x	x	x

a function of the main product characteristics, especially to the optimized variables.
These four objectives were then combined with each other in a full factorial plan in order to assess how the selection of the objective in the optimization problem may change the characteristics of the $HVAC$ optimal configurations (Table 3). For this reason, 11 optimization runs were performed for each reference building defined in previous sections.

Results

The results are a series of Pareto fronts and surfaces showing the trade-offs among the different objectives. The frequency of each optimization variable in the Pareto optimal solutions as been analyzed, since the purpose of research is to highlight the effects of the cost function selections on the optimum solutions. For this reason, the first and third quartile of any optimization variable distribution in the optimal solutions are simultaneously plotted for each optimization runs with the different choice of the cost functions. The radar plots in Figure 1 to 4 show the minimum (blue dotted line), the maximum (red dotted line), the first quartile (blue line) and the third quartile (red line) of the solutions belonging to the Pareto fronts for the main optimization variables. The surface between the red and blue line represents the range of each optimization variable, within which are contained the 50% of the optimal solutions. A detailed analysis of the effects of the cost functions on the four optimization variables with the most interesting results are presented in the following sections.

Storage Tank

Firstly, it is interesting to note the significant difference in optimum storage volume obtained for the four different buildings when only two objectives are set in the Genetic Algorithm (Figure 1a to 4a). The greater the thermal capacitance of the building envelope the lower the optimal storage volume. These results are related to the greater possibility in using the thermal inertia of the building envelope especially in well insulated and massive buildings. Similarly, the low thermal mass of the building walls also increases the variability of the storage tank volumes in the Pareto solutions. This is highlighted by the higher distances between the first (blue curve) and third quartile curves (red line).
The radar plots show also a star shapes of the curve, thus a noticeable dependence of the storage volume of the cost functions is pointed out. The introduction of the NPV in optimizations with two cost functions leads to a considerable reduction of the optimum storage volumes whatever the second objective for all the reference buildings. In these cases, the optimum volume of the 50% of the optimal solutions is between 200 and 300 liters for the case $C1$, between 50 and 250 for the $C2$, between 200 and 700 for the $T1$ and between 100 and 400 for $T2$. On the contrary, the volumes are greater in optimizations in which the two objectives are a combination of Q_h, UH and AC. In these cases, the volume of the storage tank is between 500 and 1000 liters in the 50% of the optimal solutions, for all the reference buildings. The optimal storage volumes exceed the 1000 liters in the optimization (Opt5), in which UH is minimized and AC is maximized. In fact, having a large reserve of energy is important especially when the heating system is switched on in the morning hours, when the low outdoor temperatures limits the COP and, consequently, the $ASHP$ capacity. Similarly, it is important to obtain the simultaneity of PV production with the energy consumption to maximize the AC goal. Thus, the charge of a large storage tank in the morning tends to optimize this objective, especially when this solution is combined with the east orientation of the PV modules.
Another interesting result is related to simultaneous optimization of three cost functions. The introduction of the third objective leads to similar storage solutions, except for the optimization run in which NPV is the missing goal (Opt9). In the latter case, in fact, the optimal volume within which are the 50% of the optimal solutions becomes from 500 to 1100 liters except for the $C1$ building.
Finally the optimization conducted with all the four goals leads to a volume range that is not affected by the reference building. In Opt11, the interquartile range is larger than the other optimization runs and the optimal storage volumes ranging from 400 to 900 liters, regardless to the envelope characteristics.

Battery Total Capacity

These results show a limited dependence of the interquartile range from the reference building's characteristics (Figure 1b to 4b). Weak differences are caused only by the building energy demand. The higher the building energy needs (cases $C1$ and $T1$), the greater the battery total capacity in the Pareto front solutions. This influence is more evident on the the first quartile values with respect to the third quar-

tiles. This means that the optimal solutions tend to flatten over medium-high battery capacity, thus showing a lower diversification of the front.
The cost function that obviously leads to further battery capacity is the maximization of AC. In this case, however, there is a significant variation according to the second objective considered in the optimization. If fact, the NPV limits the maximum total capacity that never exceeds $6\,kWh$ in all the buildings. This is because the NPV tends to penalize the batteries with greater Q_{batt} due to the higher initial cost. Besides, the values of Q_{batt} are frequently included between 950 and $1450\,Wh$ corresponding to about $80-120\,Ah$ in all optimizations runs. Hence, the modulation of the total battery capacity arises primarily from variation in the number of installed batteries.
Similar results were also obtained for the optimizations with three cost functions. The optimizations with the AC goal (i.e Opt8 ÷ Opt10) show very similar changes in the first and third quartiles. Generally, the 50% of the optimal solutions has a total capacity of the batteries between 2 and $6.5\,kWh$ in all the considered building configurations. Only in $T1$ the choice of Q_h, NPV and AC leads to the selection of total capacity up to $8\,kWh$. The three cost function optimization without the AC objective induces the selection of lower battery capacity, which vary between 950 and $3000\,Wh$. Finally, the optimization with four goals leads to similar results in cases with the same insulation level of the building envelope regardless the heat capacitance. In fact, the 50% of the Pareto solutions have a total capacity between 2.2 and $5.5\,kWh$ in cases with the low insulation level (i.e. $C1$ and $T1$) while $C2$ and $T2$ show a variability from 1.5 to $6\,kWh$.

ASHP Rated Capacity

The optimal size of the heat pumps are scarcely affected by the building characteristics (Figure 1c to 4c). The rated capacity of the 50% of the Pareto solutions are comprised between 4 and $5\,kW$ in most of the optimization runs regardless the insulation level and the envelope thermal capacitance.
Different results are highlighted by the dependence on the cost function selections. Notice that the introduction of the AC objective leads to an increase of the optimal $ASHP$ sizes, especially as regards the Opt3 in which AC and Q_h are simultaneously optimized. In Opt3 the third quartile is considerable increased while the first quartile remains substantially unaltered. Hence AC causes an increased dispersion of the optimal $ASHP$ rated capacity that varies between 4 and $8.4\,kW$ when the second cost function is Q_h. The competitiveness of the two optimization goals causes the greater dispersion of the rated capacity. In fact, the PV self-consumption is promoted by the worst performance of the $ASHP$ caused by the operation at a low part load ratio, while Q_h needs an operation at high part load ratio in order to reduce the energy consumption. On the contrary, the selection of AC and UH as cost functions induces a lower dispersion of the $ASHP$ rated capacity in 50% of the solutions. In fact both the indexes cause an $ASHP$ oversizing. Hence the optimal rated capacity ranges from 10 to $12.5\,kW$ for timber envelopes and it is closed to $10\,kW$ for $C1$ case. Instead, the high thermal capacitance and the insulation level in case $C2$ smooth down the variation range between 6.8 and $8.8\,kW$.
Optimizations with three goals show both a general increase of the $ASHP$ rated capacity and a greater interquartile range when the excluded cost function is either the Q_h or the NPV in timber buildings. A similar behavior is noted even in concrete buildings for the same optimization runs and also for Opt8 when UH is the unused cost function. Finally, it should be reported as the optimizations with all the four cost functions produce similar results regardless the envelope characteristics also for this optimization variable.

Number of PV strings

In the simulations we considered strings made up of 3 modules connected in series, each with an open circuit voltage of $37\,V$. The parameter optimized and diagrammed in the Figure 1d to 4d is the number of strings connected in parallel.
The shape of the radar plot highlights a similar behavior for the four test cases. Slight variations are found only in the Opt8 when Q_h, AC and NPV are the considered cost functions. In this case, there is a reduction of the value of the third quartile in well-insulated buildings (i.e. $C2$ and $T2$) with respect to the building with a less insulated envelope.
Regarding the differences in the optimization runs, the introduction of the AC obviously increases the number of PV strings in the Pareto front solutions. It should also be underlined the great dispersion in Opt6 when the NPV and AC are used. This is related to the high competitiveness of the two objectives. The maximization of self-consumption of PV production requires an increasing number of PV stings whereas the number is greatly limited by the initial cost considered in the NPV. The numbers of PV strings in the Pareto front solutions are close to the upper limit of the variable range in most of the optimizations with two goals. The only two optimization runs for which the 50% of the front solutions has a lower number of PV strings are tied to the choice of NPV with either Q_h or UH.
The Opt9 run is particularly interesting in the optimizations with three goal. In this simulation the NPV is the neglected cost function. For this optimization run, the first quartile tends to the third quartile, thus the dispersion in the number of PV stings is severely restricted. This result therefore shows how the only goal that penalizes the number of PV strings is the NPV.

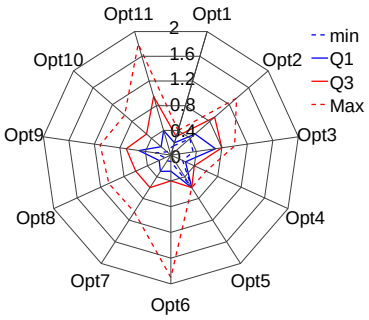

(a) Storage Tank Volume (m^3)

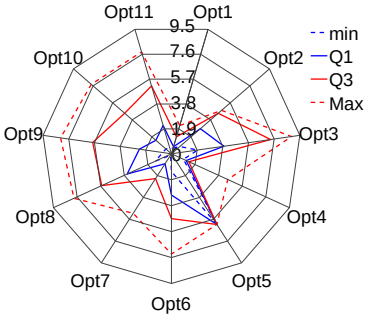

(b) Battery Total Cap. (kWh)

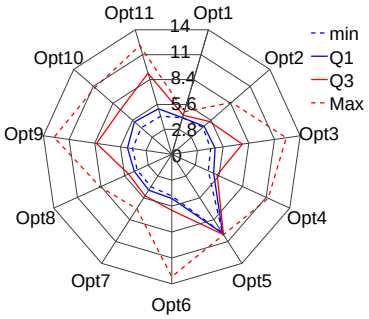

(c) ASHP rated cap. (kW)

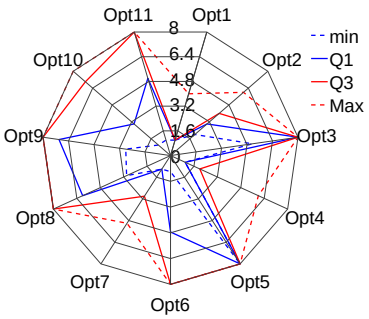

(d) PV strings ($-$)

Figure 1: Concrete envelope with low insulation (case C1)

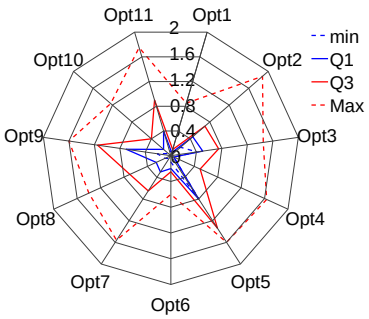

(a) Storage Tank Volume (m^3)

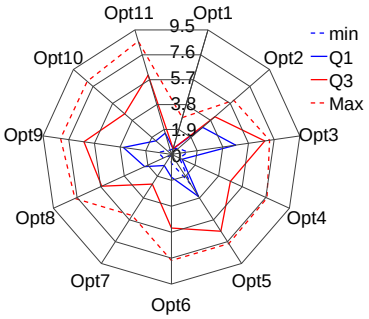

(b) Battery Total Cap. (kWh)

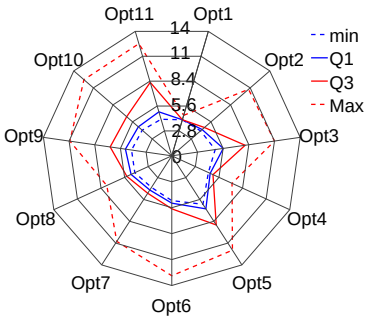

(c) ASHP rated cap. (kW)

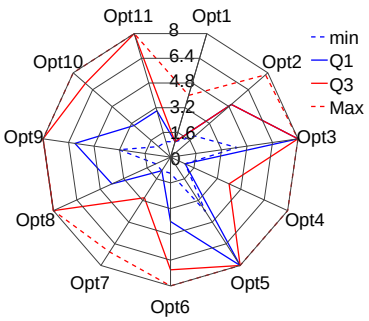

(d) PV strings ($-$)

Figure 2: Concrete envelope with high insulation (case C2)

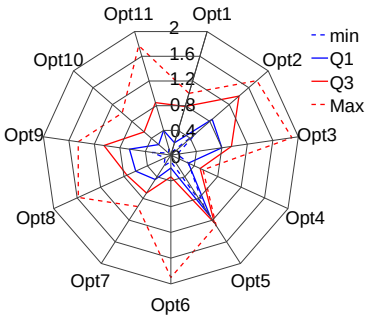

(a) Storage Tank Volume (m^3)

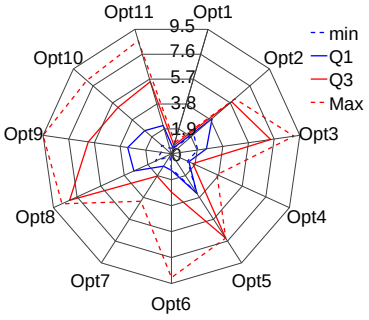

(b) Battery Total Cap. (kWh)

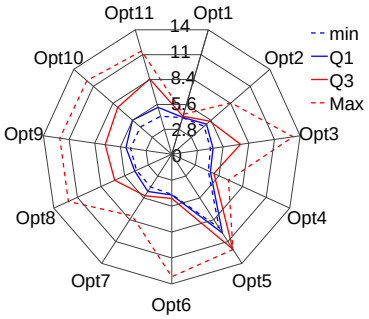

(c) ASHP rated cap. (kW)

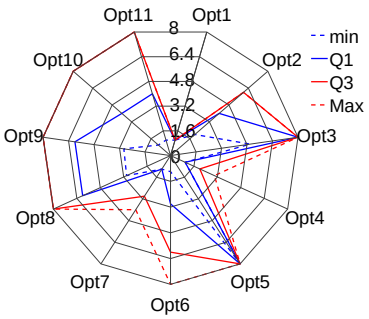

(d) PV strings (−)

Figure 3: Timber envelope with low insulation (case T1)

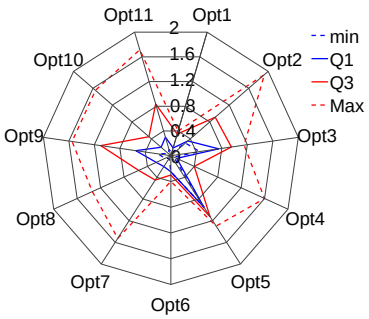

(a) Storage Tank Volume (m^3)

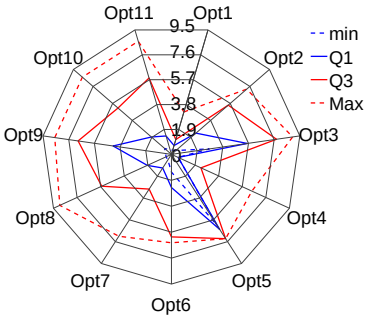

(b) Battery Total Cap. (kWh)

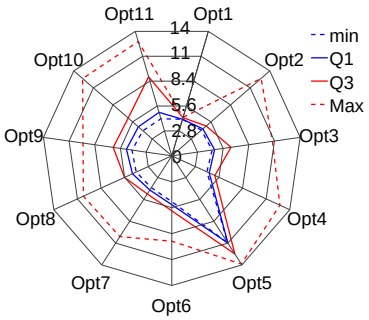

(c) ASHP rated cap. (kW)

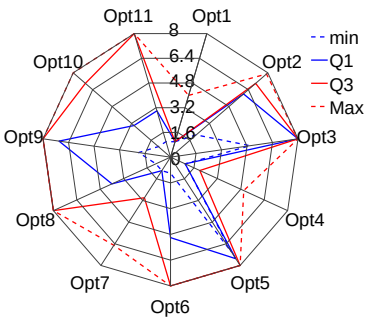

(d) PV strings (−)

Figure 4: Timber envelope with high insulation (case T2)

Finally, the front solutions obtained with the simultaneous optimization of the four cost functions show a greater dispersion of the number of PV strings. For $C2$ and $T2$, the number of strings ranges between 3 and 8 in the 50% of the optimal solutions. This ranges is restricted to 4 and 8 in $T1$ and to 5 to 8 in $C1$.

Conclusion

The paper presents an analysis on the variation of optimal HVAC design and control characteristics due to the choice of different optimization goals in the multi-objective optimization.

Firstly, the rated capacity of the $ASHP$ is scarcely affected by the choice of the cost functions. The optimum $ASHP$ size is roughly equal to $4\,kW$, whatever the choice of targets, for all the test cases used in the study. The optimization carried out with UH and AC as objectives is the only optimization run leading to an oversizing of the rated $ASHP$ capacity. This choice tends to oversize all the HVAC components as showed by the radar plots in which the storage volume, the battery total capacity and the number of PV strings are close to the upper limit of the variation range of the parameter in Opt5. Furthermore, it is observed as the first and third quartiles are generally close to each other in the Opt5 run. This implies a weak variation in the characteristics of the Pareto front solutions. Hence, UH and AC are not competing goals since they tend to favor similar solutions. These results show that the choice to maximize the renewable coverage while minimizing the hours of not meeting the internal setpoint temperature leads both to the selection of the HVAC solutions with low energy performance. These objectives are therefore strongly competing with the choice of reducing the energy consumption. This is not the case of optimization runs with the NPV goal. Even if the cost minimization could drive the decision maker toward solutions with a lower initial cost, that are also characterized by lower energy performance. This does not happen because the NPV also covers the operational costs related to the energy consumption which therefore pose a constraint to the minimum energy performance.

The use of AC and Q_h as optimization objectives leads to the choice of large storage tank, high batteries capacitance and high PV surface. The results also show that the NPV is the only objective that limits the size of the storage tanks and the number of PV modules. Thus the NPV in most of the cases is the only competitive goal with respect to the other three technical objective. Hence the limit on the size of the ideal plant components is the primary effect of the introduction of NPV in the optimization. This is also evidenced by the optimization with three objectives in which the NPV is the neglected goal. Also in this case the solutions of the front tend to maximize as far as possible the production and accumulation of energy from renewable sources.

Finally, the increasing number of cost functions tends to make the distribution of each variable in the Pareto front solutions less sensitive to either the insulation and to the thermal capacitance of the building envelope. On the contrary, the choice of only two objectives leads to the most sensitive solutions to the characteristics of the building, this especially for solutions related to the powers and plant optimum yields and the accumulation capacity requests (both thermal and electrical).

The analysis was carried out on the Pareto set containing a large number of $HVAC$ solutions by investigating the interquartile range of each variable distribution. From the building owner and/or designer perspective, the consideration of all the non-dominated solutions can be prohibitive and an inefficient task. For this reason a post Pareto analysis is required to achieve a smaller practical set, i.e the pruned Pareto front, which can be more suitable for the decision maker. In this respect, the choice of the cost functions can also affect the post Pareto results.

Nomenclature

AC	Auto-consumption of the PV production $[kWh]$
COP	Coefficient of performance $[-]$
CR	Capacity ratio according to EN 14285 $[-]$
ϕ_{rated}	Rated capacity of the ASHP $[kW]$
IC	Initial cost of the solution [€]
κ_{int}	Internal areal capacitance according to EN ISO 13786 $[kJ\,m^{-2}\,K^{-1}]$
n_{batt}	Number of batteries $[-]$
n_{str}	Number of PV strings $[-]$
NPV	Net present value [€]
$nZEB$	Nearly zero energy building $[-]$
MOO	Multi-objective optimization problem $[-]$
PMV	Fanger's predicted mean vote $[-]$
Q_1	First quartile of the variable distribution $[-]$
Q_3	Third quartile of the variable distribution $[-]$
Q_{batt}	Battery capacity $[kWh]$
Q_h	Energy consumption for heating $[kWh]$
U	Thermal transmittance according to EN ISO 6946 $[W\,m^{-2}\,K^{-1}]$
UH	Unmet hours during occupied periods $[h]$
UPS	Uninterruptible power supply $[-]$
V_{stor}	Volume of the storage tank $[m^3]$

References

2009/28/CE (2009). - council directive (EC) 28/2009 on the promotion of the use of energy from renewable sources and amending and subsequently OJ L 140/16.

Asadi, E., M. G. D. Silva, C. H. Antunes, L. Dias, and L. Glicksman (2014). Multi-objective optimization for building retrofit: A model using genetic algorithm and artificial neural network and an application. *Energy and Buildings 81*, 444–456.

Ascione, F., N. Bianco, C. De Stasio, G. M. Mauro, and G. P. Vanoli (2015). A new methodology for cost-optimal analysis by means of the multi-objective optimization of building energy performance. *Energy and Buildings 88*, 78–90.

ASHRAE 90.1 (2007). Energy standard for buildings except low rise residential buildings. Technical report, ASHRAE - American Society of Heating, Refrigerating, and Air-Conditioning Engineers, Atlanta, Georgia.

Bee, E., A. Prada, and P. Baggio (2016). Variable-speed air to water heat pumps for residential buildings: evaluation of the performance in tnorthern italian climate. In *CLIMA* 2016 - *proceedings of the* 12^{th} *REHVA World Congress, vol. 3*, Aalborg (Denmark). Aalborg University, Department of Civil Engineering.

Bichiou, Y. and M. Krarti (2011). Optimization of envelope and HVAC systems selection for residential buildings. *Energy and Buildings 43*(12), 3373–3382.

Burjorjee, K. M. (2013). Explaining optimization in genetic algorithms with uniform crossover. In *proceedings of FOGA'13 - twelfth workshop on foundations of genetic algorithms XII*, Adelaide, (Australia), pp. 37–50. ACM New York, USA.

Carlon, E., M. Schwarz, A. Prada, L. Golicza, V. K. Verma, M. Baratieri, W. Haslinger, and C. Schmidl (2016). On-site monitoring and dynamic simulation of a low energy house heated by a pellet boiler. *Energy and Buildings 116*, 296–306.

Carlucci, S., L. Pagliano, and P. Zangheri (2013). Optimization by Discomfort Minimization for Designing a Comfortable Net Zero Energy Building in the Mediterranean Climate. *Advanced Materials Research 689*(May), 44–48.

Deb, K. (2002). A fast and elitist multi-objective genetic algorithm: NSGA-II. *IEEE transactions on evolutionary computation 6*, 182–197.

Eisenhower, B., Z. O'Neill, S. Narayanan, V. A. Fonoberov, and I. Mezić (2012). A methodology for meta-model based optimization in building energy models. *Energy and Buildings 47*, 292–301.

EN 14285 (2012). Testing and rating at part load conditions and calculation of seasonal performance. Tech. stand., CEN, European Committee for Standardization.

EN 15459 (2007). Energy performance of buildings - economic evaluation procedure for energy systems in buildings. Tech. stand., CEN, European Committee for Standardization.

EN ISO 13786 (2007). Thermal performance of building components - dynamic thermal characteristics - calculation methods. Tech. stand., CEN, European Committee for Standardization.

EN ISO 6946 (2005). Building components and building elements - thermal resistance and thermal transmittance - calculation method. Tech. stand., CEN, European Committee for Standardization.

Evins, R. (2013). A review of computational optimisation methods applied to sustainable building design. *Renewable ans Sustainable Energy Reviews 22*, 230–245.

Evins, R., P. Pointer, and S. Burgess (2012). Multi-Objective optimisation of a modular building for different climate types. In *BSO12 - First Building Simulation and Optimization Conference*, Loughborough (UK), pp. 417–424.

Fesanghary, M., S. Asadi, and Z. W. Geem (2012). Design of low-emission and energy-efficient residential buildings using a multi-objective optimization algorithm. *Building and Environment 49*(1), 245–250.

Fleischer, M. (2003). The measure of pareto optima. applications to multi-objective metaheuristics. In *proceedings of EMO2003 -* 2^{nd} *International conference on Evolutionary Multi-Criterion Optimization*, Faro, Portugal, pp. 519–533. Springler.

Goldberg, D. E. and K. Deb (1990). A comparative analysis of selection schemes used in genetic algorithms. In *proceedings of FOGA1 -* 1^{st} *workshop on foundations of genetic algorithms*, Bloomington, USA, pp. 69–93. Morgan Kaufmann.

Goldberg, D. E., B. Korb, and K. Deb (1989). Messy genetic algorithms: motivation, analysis, and first results. *Complex Systems 3*, 493–530.

Hamdy, M., A. Hasan, and K. Siren (2011a). Applying a multi-objective optimization approach for Design of low-emission cost-effective dwellings. *Building and Environment 46*(1), 109–123.

Hamdy, M., A. Hasan, and K. Siren (2011b). Impact of adaptive thermal comfort criteria on building energy use and cooling equipment size using a multi-objective optimization scheme. *Energy and Buildings 43*(9), 2055–2067.

Hasan, A., M. Vuolle, and K. Sirén (2008). Minimisation of life cycle cost of a detached house using combined simulation and optimisation. *Building and Environment 43*(12), 2022–2034.

Ihm, P. and M. Krarti (2013). Design Optimization of Energy Efficient Office Buildings in Tunisia. *Journal of Solar Energy Engineering 135*(4), 1–10.

Ko, M. J., Y. S. Kim, M. H. Chung, and H. C. Jeon (2015). Multi-objective optimization design for a hybrid energy system using the genetic algorithm. *Energies 8*, 2924–2949.

Magnier, L. and F. Haghighat (2010). Multiobjective optimization of building design using TRNSYS simulations, genetic algorithm, and Artificial Neural Network. *Building and Environment 45*(3), 739–746.

Matsumoto, M. and T. Nishimura (1998). Mersenne twister: a 623-dimensionally equidistributed uniform pseudo-random number generator. *ACM Transactions on Modeling and Computer Simulation (TOMACS) 8*, 3–30.

Penna, P., A. Prada, F. Cappelletti, and A. Gasparella (2015). Multi-objectives optimization of energy efficiency measures in existing buildings. *Energy and Buildings 95*, 57–69.

Pountney, C. (2012). Better carbon saving: using a genetic algorithm to optimise building carbon reductions. In *BSO12 - First Building Simulation and Optimization Conference*, Loughborough (UK), pp. 165–172.

Prada, A., G. Pernigotto, F. Cappelletti, and A. Gasparella (2015). Impact of solar irradiation models on building refurbishment measures from multi-objective optimization. In *Proceedings of BS* 2015 - 14^{th} *International Conference of Building Simulation*, Hyderabad (India), pp. 2809–2816.

Saltelli, A., S. Tarantola, F. Campolongo, and M. Ratto (2004). *Sample generation, in Sensitivity analysis in practice. A guide to assessing scientific models*. John Wiley & Sons.

Verbeeck, G. and H. Hens (2007). Life Cycle Optimization of Extremely Low Energy Dwellings. *Journal of Building Physics 31*(2), 143–177.

Wang, W., R. Zmeureanu, and H. Rivard (2005). Applying multi-objective genetic algorithms in green building design optimization. *Building and Environment 40*(11), 1512–1525.

Wright, J., E. Nikolaidou, and C. J. Hopfe (2016). Exhaustive search; does it have a role in explorative design? In *BSO16 - Third Building Simulation and Optimization Conference*, Newcastle (UK).

Zitzler, E. and L. Thiele (1999). Multiobjective evolutionary algorithms: A comparative case study and the strength pareto approach. *IEEE Transactions on evolutionary computation 3*, 257–271.